Dendritic Spine Shape Classification from Two-Photon Microscopy Images
Dendritik Diken Şekillerinin İki Foton Mikroskopi Görüntüleri Kullanılarak Sınıflandırılması

Muhammad Usman Ghani*, Sümeyra Demir Kanık*, Ali Özgür Argunşah†, Tolga Taşdizen‡*,
Devrim Ünay§, Müjdat Çetin*
*Signal Processing and Information Systems Lab,Faculty of Engineering and Natural Sciences, Sabanci University, Istanbul, Turkey
†Champalimaud Neuroscience Programme, Champalimaud Centre for the Unknown, Lisbon, Portugal
‡Electrical and Computer Engineering Department, University of Utah, USA
§Department of Biomedical Engineering, Faculty of Engineering and Natural Sciences, Bahcesehir University, Istanbul, Turkey
{ghani,sumeyrakanik,mcetin}@sabanciuniv.edu,{ali.argunsah}@neuro.fchampalimaud.org,
{tolga}@sci.utah.edu, {devrim.unay}@eng.bahcesehir.edu.tr

***Abstract*—Functional properties of a neuron are coupled with its morphology, particularly the morphology of dendritic spines. Spine volume has been used as the primary morphological parameter in order the characterize the structure and function coupling. However, this reductionist approach neglects the rich shape repertoire of dendritic spines. First step to incorporate spine shape information into functional coupling is classifying main spine shapes that were proposed in the literature. Due to the lack of reliable and fully automatic tools to analyze the morphology of the spines, such analysis is often performed manually, which is a laborious and time intensive task and prone to subjectivity. In this paper we present an automated approach to extract features using basic image processing techniques, and classify spines into mushroom or stubby by applying machine learning algorithms. Out of 50 manually segmented mushroom and stubby spines, Support Vector Machine was able to classify 98% of the spines correctly.**

***Keywords*—Dendritic Spines, Classification, Clustering, Neuroscience.**

***Özetçe* —Sinir hücresinin işlevsel özellikleri dendrit dikenlerinin morfolojisiyle yakından ilişkilidir. Dendrit diken hacmi, yapı ve fonksiyon arasındaki ilişkiyi anlamak için kullanılan temel morfolojik parametredir. Fakat bu indirgemeci yaklaşım dikenlerin zengin şekil repertuvarını ihmal etmektedir. Diken şekil bilgisini fonksiyonu ile ilişkilendirmenin ilk adımı dikenleri literatürde önerilen temel şekil gruplarına göre sınıflandırmaktır. Diken morfolojisini inceleyen güvenilir ve tamamen otomatik bir aracın bulunmaması analizlerin insanlar tarafından el ile yapılmasına yol açmaktadır. Bu da yorucu, zaman alan bir ugraştır ve subjektif sonuçlar ortaya çıkarmaktadır. Bu çalışmada temel görüntü işleme tekniklerini kullanarak dikenlerden öznitelik çıkarmayı ve makine öğrenme algoritmaları ile dikenleri mantar ya da güdük olarak sınıflandırmayı öneriyoruz. El ile bölütlenmiş mantar ve güdük gruplarından oluşan toplam 50 diken, Destek Vektör Makineleri kullanılarak %98 doğruluk payıyla sınıflandırılmıştır.**

***Anahtar Kelimeler*—Dendritik dikenler, sınıflandırma , kümeleme, sinirbilim.**

I. Introduction

Dendritic spines, small bulbous protrusions of the dendrites, are one of the few salient features of neurons and have been imaged and widely studied in the last century. Ramon y Cajal first identified spines in the 19th century; and suggested that changes in neuron activity might cause variations in spines morphology [1]. Studies verified that different neuron activities affected spine morphology and density [2]. Analysis of spine morphology is of significant importance in neurobiological research and can enable neuroscientists to deduce the underlying relationship between spine morphological changes and neuron activities [1]. Considering its importance, quantitative analysis of spine morphology has become a major topic of interest in contemporary neuroscience.

In the literature, dendritic spines are classified into four types: mushroom, stubby, thin and filopodia [3]. But there is an ongoing discussion whether distinct spines classes exist or there is a continuum of shapes. Arellano et al. [4] suggested that there were no clearly distinguished shape classes. There were some intermediate shapes in data studied by Peters et al. [5]. In a study conducted by Spacek et al. [6], intermediate classes were found between mushroom and thin, and mushroom and stubby. The major reason of dispute is argued to be lack of standard criteria for classification of shapes [7]. Nevertheless, existence of continuum of shapes persists to be an open question. According to Parnass et al. [8], classification of spine morphologies do not depict in itself different classes of spines, but it presents various shapes that a spine can adapt at different times.

Automated analysis of spine morphology would assist neuroscientists and accelerate the analysis process. This research aims to develop an automated analysis algorithm to classify spines from Two-Photon Laser Scanning Microscopy (2PLSM) images. The images are projected to 2D before applying image processing algorithms. We have developed procedures to extract features that are informative about the spine shape classes. Basic image processing and machine learning techniques are applied to classify spines. In order to perform evaluation , output of the classification on segmented images is compared with labels assigned by an expert. Results validate that performance of the developed approach is comparable to that of a human expert.

The rest of this paper is organized as follows: Section II presents a brief overview of literature, methodology is described in Section III, results are presented in Section IV and Section V contains conclusions as well as suggestions for future work.

978-1-4799-4874-1/14/$31.00

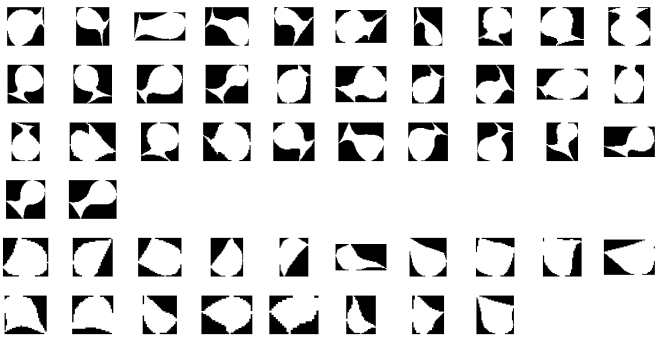

Figure 1: Data-set consists of mushroom (examples above) and stubby (below) spines

II. Literature Review

Although many different algorithms are proposed to segment the dendritic spines automatically, there are a few studies in the literature focused on automated classification of dendritic spines. Rodriguez et al. [9] conducted a study on 3D images acquired by confocal laser scanning microscopy (CLSM) and calculated aspect ratio, head to neck ratio, head diameter, and neck length as features. They employed a decision tree for classification and validated the results using the manual analysis by human expert operators to validate results. Inter-operator and intra-operator variability was reported in this study.

Son et al. [10] utilized head diameter, neck diameter, length, shape criteria, area (number of foreground pixels) and perimeter to classify spines with the decision tree classification algorithm. Images were collected using CLSM. This study also used manual analysis to evaluate their results. Koh et al. [11] used the ratio of head diameter to neck diameter to classify spines from 2PLSM images with a rule based classifier. Shi et al. [12] proposed a weighted 3D feature set including head diameter, neck diameter, length and volume for classification of spines from CLSM images.

Most of these studies focus on CLSM images, whereas only a few studies are reported on 2PLSM images. Rule based classification algorithms are commonly applied in these studies and the impact of different features is not reported. This research attempts to fill this gap in the literature.

III. Methodology

This section describes the data and methodology of the proposed approach. Mice post natal 7 to 10 days old animals are imaged every 5 minutes using 2PLSM.[1] Seven stacks of 3D images are acquired. Images are projected to 2D using Maximum Intensity Projection (also known as Maximum Activity Projection). The spines are manually segmented and labeled by an expert from 2D images. The dataset used for this research includes 50 spines from 7 images, 32 are mushroom and 18 are stubby spines. The manually segmented spines are presented in Figure 1. Stubby spines have short necks with respect to other classes. Mushroom type spines have big heads with relatively longer necks. Therefore neck length and head diameter are considered important features to identify these classes.

[1] All animal experiments are carried out in accordance with European Union regulations on animal care and use, and with the approval of the Portuguese Veterinary Authority (DGV).

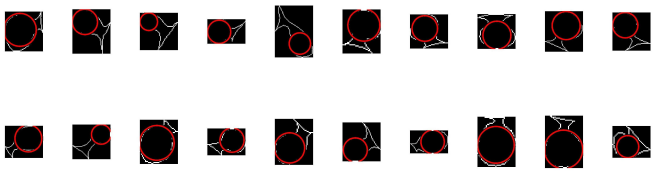

Figure 2: Circle fitting results

The features used in this study are listed below:

- Head Diameter
- Neck Length
- Area (No. of Pixels in foreground)
- Perimeter
- Height of bounding box
- Width of bounding box
- Neck Length to Head Diameter Ratio
- Circularity
- White to Black Pixels ratio in bounding box
- Shape Factor

In order to compute the head diameter, Hough Circle Transform (HCT) [13] is applied to fit the biggest circle inside the spine. For some of the spines, HCT fails to fit a circle in the spine head. In this case, the ellipse fitting algorithm of [14] is applied. Finally head diameter is computed from the diameter of the circle or the axes of the ellipse fitted in the spine head. The results of the circle fitting algorithm are presented in Figure 2 for some of the spines.

Circularity is computed using perimeter and area as shown in Equation 1.

$$Circularity = \frac{Perimeter^2}{4\pi \times Area} \tag{1}$$

Neck length computation is a challenging process. First, dendrite perimeter and medial axis are extracted from maximum intensity projection image, to be used at later stage as reference point. First we applied Otsu thresholding to get a rough segmentation of the dendrite (which included spines as well), and skeletonized this segment using a fast marching distance transform approach [15]. Then in order to exclude spines from the dendrite we applied erosion with a locally-adaptive sized, disk-shaped structuring element that runs over the medial axis. To achieve size variation, at every medial axis location diameter of the structuring element was adapted to the measured width of the segment.

Based on manual analysis of stubby spines, a heuristic is applied, if the circle fitted on spine head intersects with dendrite, it is concluded that the spine does not have a neck. Otherwise, neck length computation algorithm is applied. Then the algorithm computes the distance from spine boundary points to the center of head, and selects top N points with maximum distance. Subsequently the distance is calculated between sorted spine points and dendrite medial axis. A threshold (T_m, maximum allowed distance) is applied to the distance between these N points and the dendrite medial axis. T_m is computed as follows: $T_m = meanDistance + 2 \times StandardDeviation$, where $meanDistance$ and $StandardDeviation$ represent mean and standard deviation of distance from each sorted spine

Figure 3: Shortest Paths for Neck Length Computation

point to dendrite medial axis respectively. Pixels below T_m are selected as candidate pixels for base points. Base points are the pixels where the spine is connected to the dendrite surface. This approach allows us to locate the pixels closest to the dendrite and furthest from the spine head.

Among the candidate pixels, the two pixels with maximum distance from each other under the condition distance $\leq 3 \times headRadius$ are selected to be the base pixels of the spine, here $headRadius$ represent radius of spine head. Finally, Multistencil Fast Marching (MSFM) method [16] is used to construct a distance map. This map is used as an input for the Runge-Kutta algorithm [17] to calculate the shortest path between center point of the spine head and the target point (center point between base pixels). Shortest path results for neck length computation for a few images are depicted in Figure 3. Neck length is measured by subtracting the radius of the head from shortest path length ($Dist$ = shortest path length):

$$NeckLength = Dist - headRadius \quad (2)$$

To compute shape factor, which consists of three features, the algorithm fits a circle inside the bounding box of the spine with $radius = (NeckLength + HeadDiameter)/2$. Then white pixels inside the circle, white pixels outside the circle, black pixels inside the circle are calculated and serve as the three features of the shape factor.

New let us turn to the problem of designing and evaluating a classifier. Three different classifiers are applied: C4.5 decision tree [18], Single perceptron neural network [19] and Support Vector Machines (SVM) classifier with linear kernel [20]. Classifier performance is evaluated using 3-Fold cross-validation.

Considering the nature of this problem, quite often human experts are not available to provide manual labels, therefore it is interesting to look at this problem from a clustering perspective as well. For this purpose, K-means clustering algorithm [21] is also used, and its results are discussed in the next section.

IV. Results

Experiments have been conducted with the full feature set first. To study the role of individual features on classification performance, we conduct experiments with a selected subset of the features as well. To validate results, class labels have been acquired by the assistance of a human expert.

A. Experiment 1: All Features

This experiment uses all features for classification and clustering. As stated earlier, 3-fold cross-validation is applied to validate classification results. The results of classification for different classifiers are presented in Table I. While all three classifiers are able to identify mushroom spines accurately, decision tree fails to classify 33% of the stubby spines. For K-means clustering, performance is evaluated for 2 and 3

Table I: Experiment 1 Classification Results

Classifier	Mushroom	Stubby	Overall
C 4.5 Decision Tree	96.88%	66.67%	86.00%
Neural Network	96.88%	94.44%	96.00%
SVM	96.88%	94.44%	96.00%

Table II: Experiment 1 Clustering results with 2 Clusters

Class	Cluster 1	Cluster 2	Accuracy
Mushroom	17	15	53.13%
Stubby	0	18	100%
Overall			70%

clusters and the results are given in Table II and Table III respectively. Results in Table II exhibit a huge overlap between mushroom and stubby spines. When we allow 3 clusters, one mushroom and one stubby cluster are formed with a third cluster containing samples from both classes. The third cluster including samples from both classes can be analyzed by human experts to group them into stubby or mushroom. We may conclude that, manual effort required by human experts is reduced using clustering scheme as compared to entirely manual analysis.

B. Experiment 2: Selected Features

In this experiment, we use only two features: head diameter and neck length of the spines. These features are selected because they are the most discernible parameters for mushroom and stubby spines. Scatter plot of these two features is shown in Figure 4. With only two features, all classifiers are able to recognize both mushroom and stubby spines as it can be seen in Table IV. This performance is expected, as the scatter plot of the two features show a clear distinction between two classes in Figure 4.

Results of k-means clustering with two features for k=2 are similar to the previous experiment as seen in Table V.

Table III: Experiment 1 Clustering results with 3 Clusters

Class	Cluster 1	Cluster 2	Cluster 3	Accuracy
Mushroom	17	15	0	100%
Stubby	0	9	9	50%
Overall				82%

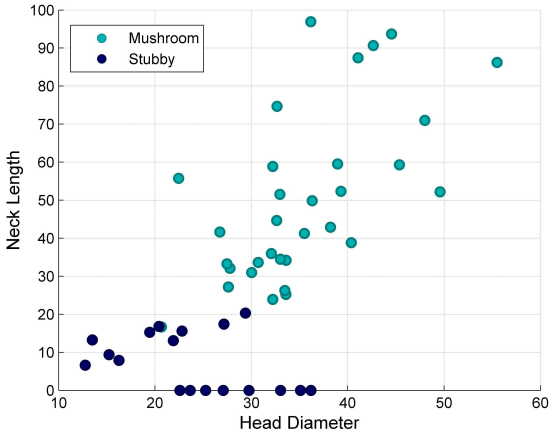

Figure 4: Mushroom and Stubby spines have distinguishable feature distribution

Table IV: Experiment 2 Classification Results

Classifier	Mushroom	Stubby	Overall
C 4.5 Decision Tree	96.88%	94.44%	96.00%
Neural Network	96.88%	94.44%	96.00%
SVM	96.88%	100.00%	98.00%

Table V: Experiment 2 Clustering results with 2 Clusters

Class	Cluster 1	Cluster 2	Accuracy
Mushroom	19	13	59.38%
Stubby	0	18	100%
Overall			74%

For k=3 clusters, however, we see two mushroom clusters and one stubby cluster with only one spine misplaced (Table VI). This mushroom spine erroneously clustered as stubby has been misclassified as well. The particular spine is a small mushroom type spine with short neck length which causes the confusion (Figure 5).

V. Conclusion

Dendritic spine morphology is highly regulated by the activity it receives. Currently manual analysis is often used to study morphological changes in spines. Availability of automated analysis would accelerate the analysis process. This research is an effort to achieve this goal. Two-photon microscopy images has been used to conduct this study, and the effectiveness of the use of different shape based features is tested. It is verified that neck length and head diameter are promising features to classify mushroom and stubby spines. It is also concluded that clustering can be used in this context to group data into different number of clusters and to reduce the effort required for manual analysis. Data size used for this research is small, and thin and filopodia type spines are not included. One main reason is the time-intensive data acquisition process. It requires human experts involvement to manually segment and assign class labels. For future work, we are planning to increase data size and include other type of spines as well.

ACKNOWLEDGEMENT

This work has been supported by the Scientific and Technological Research Council of Turkey (TUBITAK) under Grant 113E603 and by a TUBITAK-2221 Fellowship for Visiting Scientists and Scientists on Sabbatical Leave. The authors would also like to thank the Neuronal Structure and Function Lab, Champalimaud Centre for the Unknown (Portugal), for providing the data used in this research.

Table VI: Experiment 2 Clustering results with 3 Clusters

Class	Cluster 1	Cluster 2	Cluster 3	Accuracy
Mushroom	21	10	1	96.88%
Stubby	0	0	18	100%
Overall				98%

Figure 5: Mis-classified Mushroom Spine

References

[1] J. Lippman and A. Dunaevsky, "Dendritic spine morphogenesis and plasticity," *Journal of neurobiology*, vol. 64, no. 1, pp. 47–57, 2005.

[2] R. Yuste and B. T., "Morphological changes in dendritic spines associated with long-term synaptic plasticity." *Annu Rev Neurosci*, vol. 24, p. 1071–1089, 2001.

[3] F. Chang and W. T. Greenough, "Transient and enduring morphological correlates of synaptic activity and efficacy change in the rat hippocampal slice," *Brain Res.*, vol. 309, p. 35–46, 1984.

[4] J. I. Arellano, R. Benavides-Piccione, J. DeFelipe, and R. Yuste, "Ultrastructure of dendritic spines: correlation between synaptic and spine morphologies," *Frontiers in neuroscience*, vol. 1, no. 1, 2007.

[5] A. Peters and I. R. Kaiserman-Abramof, "The small pyramidal neuron of the rat cerebral cortex. the perikaryon, dendrites and spines," *Am. J. Anat.*, vol. 127, p. 321–356, 1970.

[6] J. Spacek and M. Hartmann, "Three-dimensional analysis of dendritic spines. i. quantitative observations related to dendritic spine and synaptic morphology in cerebral and cerebellar cortices," *Anat. Embryol.*, vol. 167, p. 289–310, 1983.

[7] B. Ruszczycki, Z. Szepesi, G. M. Wilczynski, M. Bijata, K. Kalita, L. Kaczmarek, and J. Wlodarczyk, "Sampling issues in quantitative analysis of dendritic spines morphology." *BMC Bioinformatics*, vol. 13, p. 213, 2012.

[8] Z. Parnass, A. Tashiro, and R. Yuste, "Analysis of spine morphological plasticity in developing hippocampal pyramidal neurons," *Hippocampus*, vol. 10, p. 561–568, 2000.

[9] A. Rodriguez, D. B. Ehlenberger, D. L. Dickstein, P. R. Hof, and S. L. Wearne, "Automated three-dimensional detection and shape classification of dendritic spines from fluorescence microscopy images," *PloS one*, vol. 3, no. 4, 2008.

[10] J. Son, S. Song, S. Lee, S. Chang, and M. Kim, "Morphological change tracking of dendritic spines based on structural features," *Journal of microscopy*, vol. 241, no. 3, pp. 261–272, 2011.

[11] I. Y. Koh, W. B. Lindquist, K. Zito, E. A. Nimchinsky, and K. Svoboda, "An image analysis algorithm for dendritic spines," *Neural computation*, vol. 14, no. 6, pp. 1283–1310, 2002.

[12] P. Shi, X. Zhou, Q. Li, M. Baron, M. A. Teylan, Y. Kim, and S. T. Wong, "Online three-dimensional dendritic spines mophological classification based on semi-supervised learning," in *ISBI'09 IEEE International Symposium on Biomedical Imaging: From Nano to Macro. (pp. 1019-1022)*, 2009.

[13] T. Atherton and D. Kerbyson, "Size invariant circle detection." *Image and Vision Computing*, vol. 17, no. 11, pp. 795–803, 1999.

[14] Y. Xie and Q. Ji, "A new efficient ellipse detection method," in *16th International Conference on Pattern Recognition*, vol. 2, 2002, pp. 957–960.

[15] R. V. Uitert and I. Bitter, "Subvoxel precise skeletons of volumetric data based on fast marching methods," *Medical Physics*, vol. 34, no. 2, pp. 627–638, 2007.

[16] M. Hassouna and A. Farag, "Multistencils fast marching methods: A highly accurate solution to the eikonal equation on cartesian domains," *Pattern Analysis and Machine Intelligence, IEEE Transactions on*, vol. 29, no. 9, pp. 1563–1574, Sept 2007.

[17] J. C. Butcher, *The Numerical Analysis of Ordinary Differential Equations: Runge-Kutta and General Linear Methods*. New York, NY, USA: Wiley-Interscience, 1987.

[18] J. R. Quinlan, *C4.5: Programs for Machine Learning*. San Francisco, CA, USA: Morgan Kaufmann Publishers Inc., 1993.

[19] S. Haykin, *Neural Networks: A Comprehensive Foundation*, 2nd ed. Upper Saddle River, NJ, USA: Prentice Hall PTR, 1998.

[20] C.-C. Chang and C.-J. Lin, "Libsvm: A library for support vector machines," *ACM Trans. Intell. Syst. Technol.*, vol. 2, no. 3, pp. 27:1–27:27, May 2011.

[21] D. Arthur and S. Vassilvitskii, "K-means++: The advantages of careful seeding," in *Proceedings of the Eighteenth Annual ACM-SIAM Symposium on Discrete Algorithms*, ser. SODA '07. Philadelphia, PA, USA: Society for Industrial and Applied Mathematics, 2007, pp. 1027–1035.